



# Cylindrical air spaced high gain dielectric resonator antenna for ultra-wideband applications

SACHIN KUMAR YADAV\*<sup>ID</sup>, AMANPREET KAUR and RAJESH KHANNA

Electronics and Communication Engineering Department, Thapar Institute of Engineering and Technology (Deemed to be University), Badson Road, Patiala, India  
e-mail: yadav\_sachinyadav@yahoo.com

MS received 27 July 2019; revised 16 May 2020; accepted 29 May 2020

**Abstract.** A new geometry of ultra-wideband (UWB) hollow dielectric resonator antenna (DRA) has been designed, simulated, and fabricated. The antenna consists of a rectangular dielectric resonator and excited by a transformer type microstrip feedline. A hollow cylindrical-shaped structure is extracted from a rectangular DR to improve the gain and impedance bandwidth of the antenna. The present work shows that the shifting within the UWB range along with the gain enhancement is observed by increased diameter of the hollow structure and the use of defective ground structure in the ground plane. The antenna provides four different radiating modes, namely  $TE_{11\delta}$  at 3.8 GHz,  $TE_{22\delta}$  at 6.4 GHz,  $TE_{231}^Z$  at 8.8 GHz, and  $TE_{33\delta}$  at 10 GHz that support to give wide impedance bandwidth. The simulated and measured results are in good agreement as an impedance bandwidth of 104.09% (3.28 to 10.4 GHz) and 103.86% along with a peak gain of 7.2 dB.

**Keywords.** Hollow cylindrical dielectric; quarter wave fed; rectangular dielectric resonator antenna; metallic strips; defective ground structure.

## 1. Introduction

The Ultra-Wideband (UWB) systems have gained enormous importance in the past two decades. It is implemented for both academic and industrial communities of the telecommunication applications. The Federal Communications Commission (FCC) has declared an impedance bandwidth of 7.5 GHz, i.e., from 3.1 GHz to 10.6 GHz in 2002 [1, 2]. There are several advantages of UWB communication systems as compared to others, which makes them, an excellent candidate by giving an effective solution for wireless applications.

On the other hand, dielectric resonators (DR) have been applied in the microwave circuits design such as oscillators and filters due to their high Q-factor characteristic. Moreover, it is found that the DR with low dielectric constant can be used in antenna design as a radiating element because of their low radiating Q factor. Since the last two decades, dielectric resonator antennas (DRA) have received agreeable consideration for UWB antennas due to remarkable characteristics such as simple excitation mechanisms, high radiation efficiency, nearly constant gain, compact antenna size, wider bandwidth, and ease of excitation [3, 4]. It also has the advantages of no conductive and surface wave losses. Among various shapes of the reported DRA, the rectangular DRA has received much

attention due to its mechanical simplicity [5]. Also, it provides more degree of freedom in the parametric selection. The solid DRA was exclusively studied in the early years until the hollow DRA was proposed in 1993 [6–8]. By introducing the hollow region, the effective dielectric constant and Q-factor of the DRA can be decreased, which further enhances the impedance bandwidth and gain of the antenna.

In this article, a hollow DR excited by transformer type microstrip feedline covering 3.28 to 10.4 GHz of the UWB band is proposed. It is used Rogers RT 5880 as substrate material, and partial ground having a Defective ground structure (DGS) printed on the bottom side of the substrate. Further, the two metallic rectangular strips on the bottom layer to provide stable gain and return loss of the designed antenna. Further, the antenna near field is defined by existing modes  $TE_{11\delta}$  at 3.8 GHz,  $TE_{22\delta}$  at 6.4 GHz,  $TE_{231}^Z$  at 8.8 GHz, and  $TE_{33\delta}$  at 10 GHz. The first mode is dominant, and other three are higher-order modes to support the wide impedance bandwidth.

## 2. Antenna configuration

Figures 1A, B show the simulated and fabricated view of the proposed antenna. Inspired by the hollow-shaped DRA in [7, 8] is used for wideband application. A cylindrical shaped DR having a radius of  $D_1 = 6$  mm is cut out from rectangular

\*For correspondence  
Published online: 26 June 2020

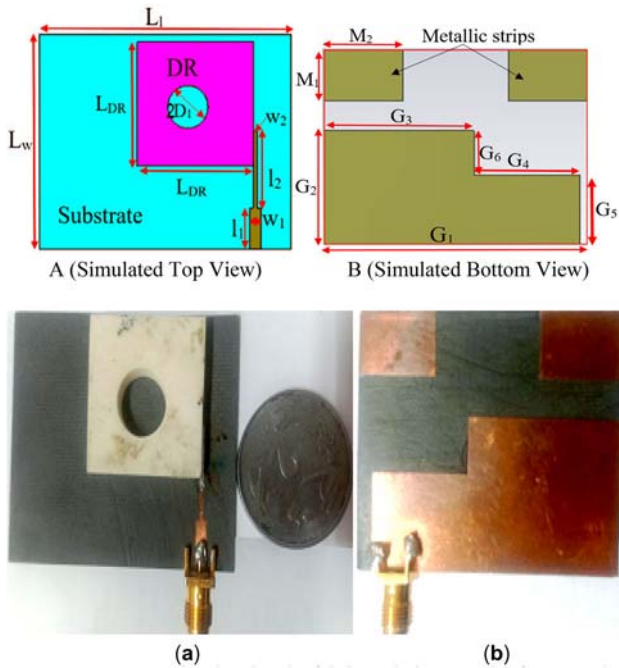


**Figure 1.** Antenna simulated and a fabricated photograph of proposed hollow antenna. A. Top view and B. back view.

DR for enhancement of both gain and impedance bandwidth of the antenna, VSWR and gain of the antenna are shown by figure 2. The DR having  $Al_2O_3$  with  $\epsilon_{dr} = 9.8$ , height  $h_{dr} = 4$  mm, excited by a quarter-wave transformer type fed printed on top of the substrate (Rogers RT 5880,  $\epsilon_s = 2.2$ , height  $h_s = 0.8$  mm) and bottom layer of the substrate has a partial ground plane with a rectangular-shaped DGS and two metallic strip  $M_2 \times M_1$  are provided stable S11 of the antenna within the UWB range. All optimized dimensions of the DRA are presented in table 1.

### 3. Simulated and experimental results

The concept of hollow DRA for the UWB range is validated in the proposed design. The proposed antenna has a dimension of  $50 \times 40 \times 4.87$  mm<sup>3</sup> simulated and fabricated. Figure 2 shows the simulated parametric results of hollow DR and the optimized value of  $D1 = 6$  mm. If hollow

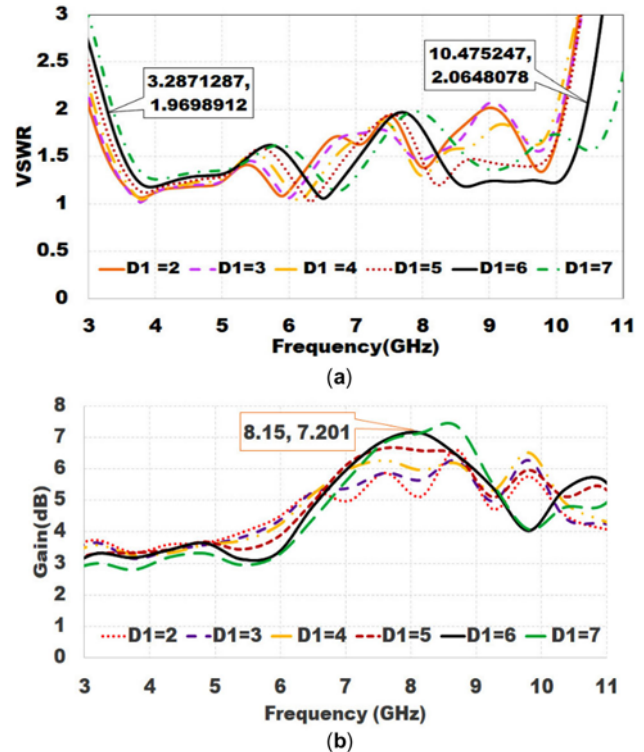


**Figure 2.** Effect of Hollow DR antenna A. VSWR, B. Gain.

diameter increases than antenna gain are improved. The hollow DR directly affects the impedance bandwidth and gain of the antenna, shown in figures 2A, B.

#### 3.1 DGS of antenna evolution steps with parametric sweep

The three structure of DRA is presented in figure 3A as Ant.1, Ant.2, and Ant.3 respectively. All antennas are used for wideband applications, Ant.1 have without DR and show the parametric sweep of  $D6$ , shown in figure 3B Ant.1. It has optimized the value of  $D6 = 9.2$  ( $-5.8$  to  $3.4$ ). Ant.2 has a DR with DGS slot  $D6$ , shown in figure 3B. This antenna gives a frequency range from  $3.6$  to

**Table 1.** Optimized parameters of the proposed DRA.

Parameters	$L_1$	$L_w$	$L_{DR}$	$l_1$	$l_2$	$w_1$	$w_2$
Values (mm)	50	40	23	7.7	14.4	2.2	0.75
Parameters	$G_1$	$G_2$	$G_3$	$G_4$	$G_5$	$G_6$	$M_2/M_1$
Values (mm)	48.5	23.4	28.5	21.5	14.2	9.2	15/10.5

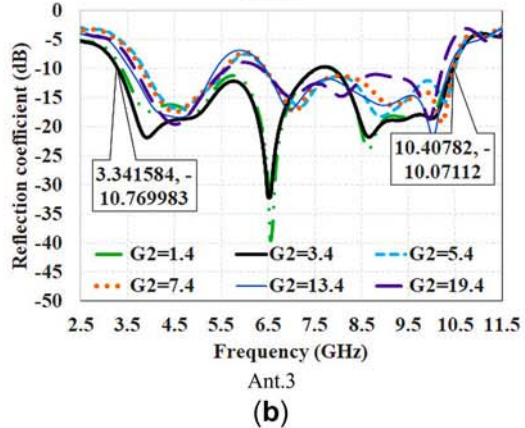
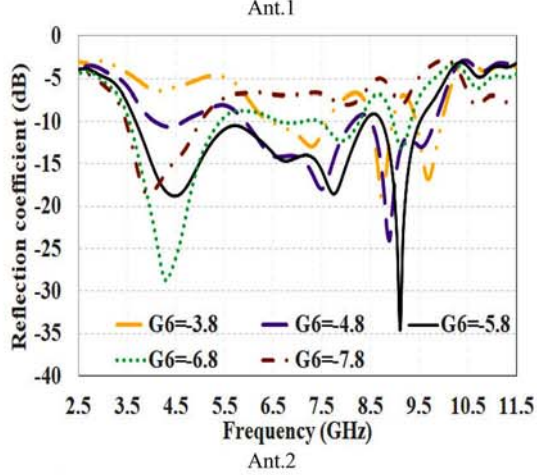
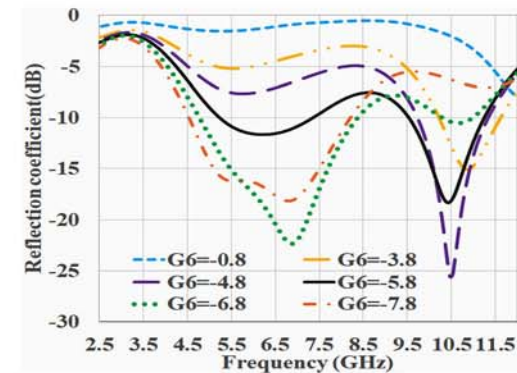
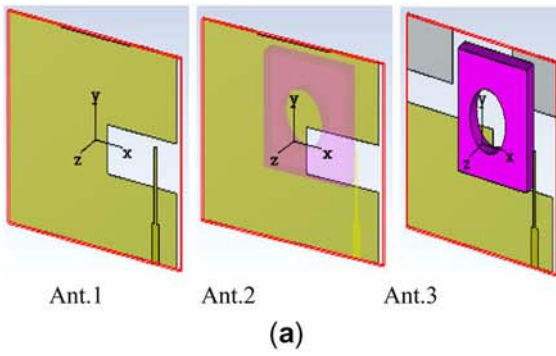


**Figure 3.** A. Antenna DGS evolution steps. B. S11 of Ant.1, Ant.2, and Ant.3.

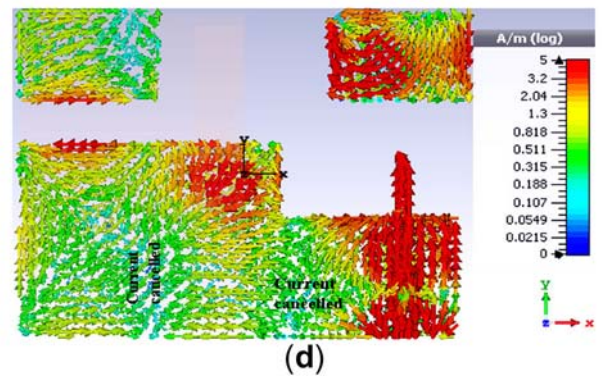
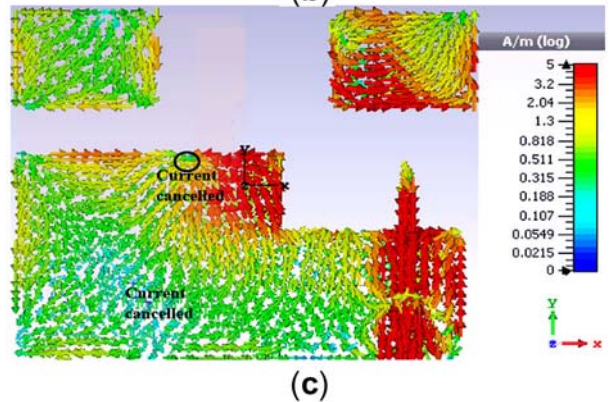
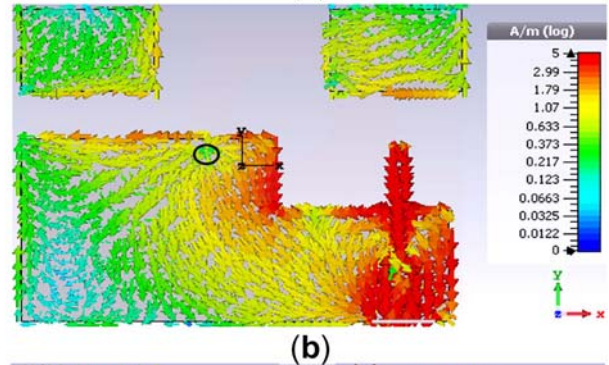
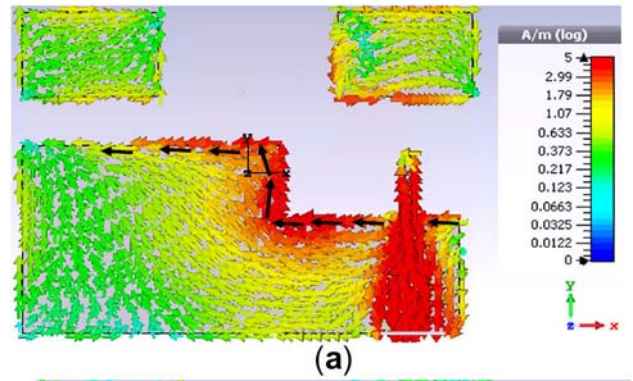


**Figure 4.** Surface current distribution at A 3.8 GHz, B 6.4 GHz, C 8.8 GHz, D 10 GHz.

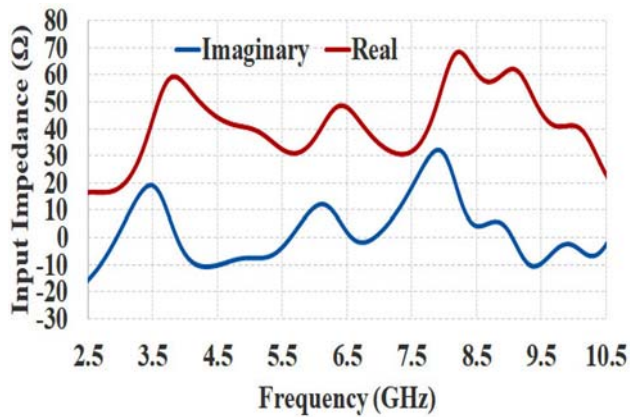


**Figure 5.** Simulated Antenna impedance plot.

9.6 GHz that is wider than Ant.2. Due to the effect of DR placed on top of the substrate layer. So, it can be observed that DR is given wider impedance bandwidth. Ant.3 has optimized dimension G2 to achieve the UWB region. The parametric sweep applies on D2 and achieves the best value 23.4 (−20 to 3.4), at this value DRA is given UWB range from 3.28 to 10.4 GHz, shown in figure 3B Ant.3.

### 3.2 Surface current distribution

The current distribution of the metallic part of the antenna is presented in figures 4A-D. The rotation of the current is observed from the surface current distribution on the ground plane as shown in figure and also, it can be observed that the decoupling structure provided the maximum surface current on the edges of the decoupling rectangular slot with different frequencies. At frequency 3.8 GHz, current directions on the x-axis shown in figure 4A. Figure 4B shows the current cancelled with a single resonance path and figure 4C-D show multiple places in ground current canceled and provide multiple resonance path with supporting of higher-order modes.

### 3.3 Modes and E-field distribution

Figure 5 shows the real and imaginary part of the impedance of the proposed UWB DRA. It is observed from figure that four maximum peaks with real values of impedance and touching the same at zero values of imaginary impedance at the frequencies of 3.8, 6.4, 8.8, and 10 GHz in the desired frequency band. To gain insight into the resonant modes at these four frequencies [9], the electric field distribution [10–16] model is depicted in figures 6A-L.

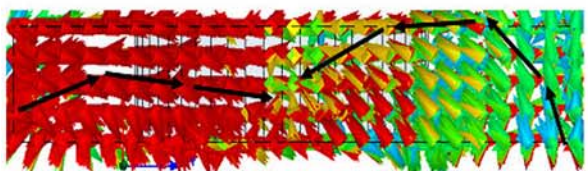
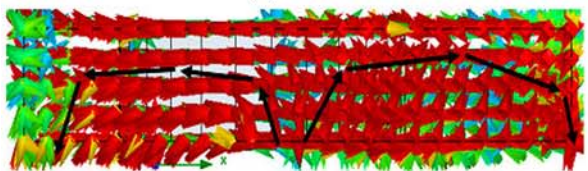
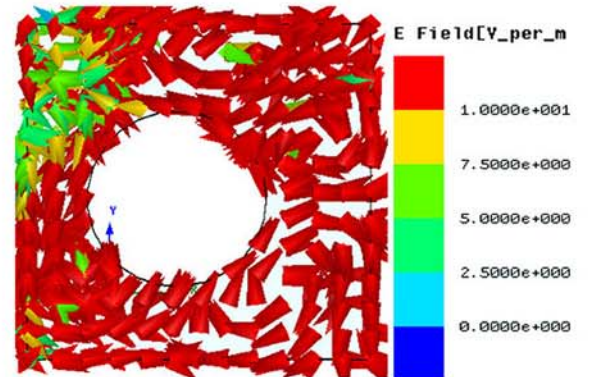
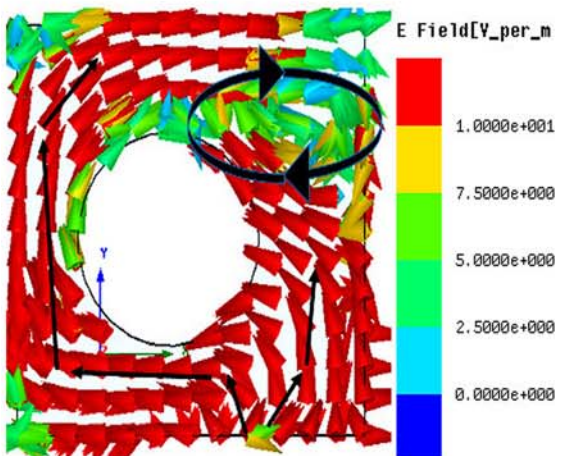
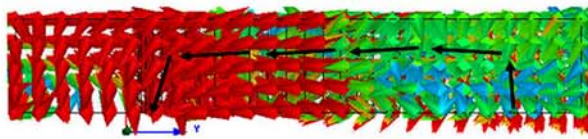
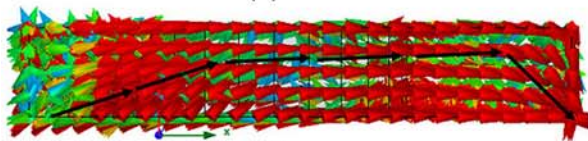
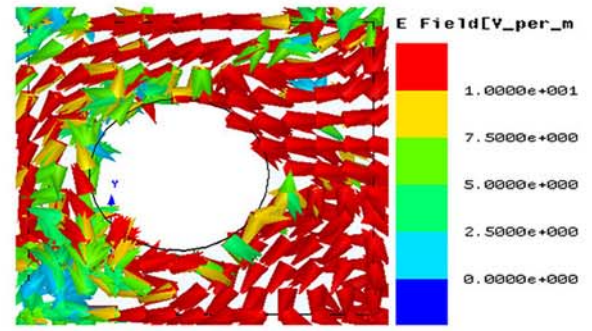
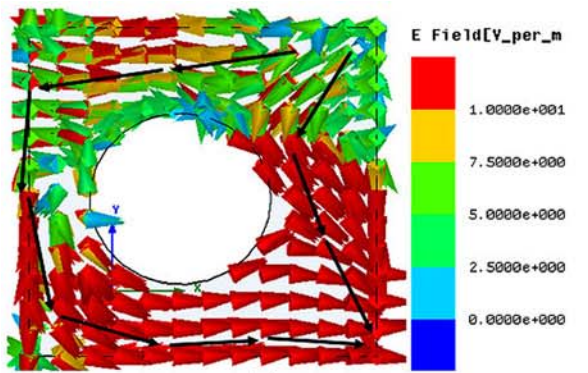
The near field depicted on the surface of DR is given in figure 6 with lower side existing fundamental mode  $TE_{11\delta}$  at 3.8 GHz in figures 6A, B, C with XY, XZ, and YZ plane, respectively. In the higher frequency side, it supports higher-order modes of  $TE_{22\delta}$  at 6.4 GHz in figures 6D, E, F with XY, XZ, and YZ plane, respectively,  $TE_{231}^Z$  at 8.8 GHz in figures 6G, H, I with XY, XZ, and YZ plane, respectively, and  $TE_{33\delta}$  at 10 GHz in figures 6J, K, L with XY, XZ, and YZ plane, respectively. These modes support wider impedance bandwidth.

### 3.4 Simulated and measured results

The simulated and measured impedance bandwidth is 104.09% (3.28–10.4 GHz), 103.86% (3.23–10.21 GHz) with peak gain 7.42 dBi, and simulated radiation efficiency is 97.6% at 4.9 GHz, as shown in figures 7 and 8. In figures 9A, B, C the simulated and measured co and cross-polarization plots for the E plane of the antenna, at three different frequencies, i.e., 4.1, 6.2, and 8.1 GHz have been described. The radiation pattern has shown that the DRA radiates properly in all directions within the desired UWB band, further the cross-polarization level is observed to be lesser than the co-polarization level.

## 4. Conclusion

In this article, a new UWB hollow dielectric resonator antenna has been designed and fabricated. Gain enhancement has been achieved by using a hollow concept, in which a cylinder with the same height of DR is extracted from the rectangular DR. The simulated results are obtained by using CST microwave studio with good agreement



◀ **Figure 6.** Near field distribution on hollow shaped DR at 3.8 GHz TE<sub>11δ</sub> A. X-Y plane B. X-Z plane C. Y-Z plane, at 6.4 GHz TE<sub>22δ</sub> D. X-Y plane E. X-Z plane F. Y-Z plane, at 8.8 GHz TE<sub>231</sub><sup>Z</sup> G. X-Y plane H. X-Z plane I. Y-Z plane, at 10 GHz TE<sub>33δ</sub><sup>Z</sup> J. X-Y plane K. X-Z plane L. Y-Z plane.

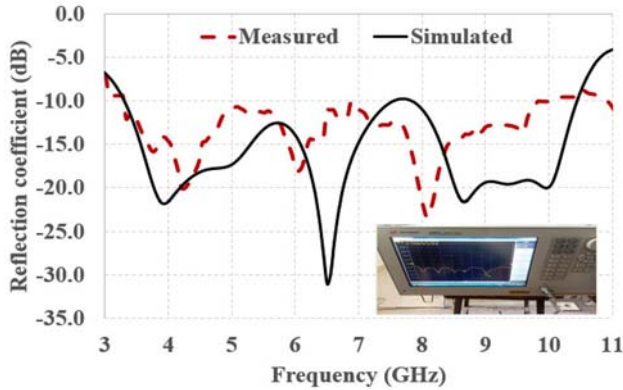


**Figure 7.** Simulated and measured S-parameter of the proposed hollow DRA.

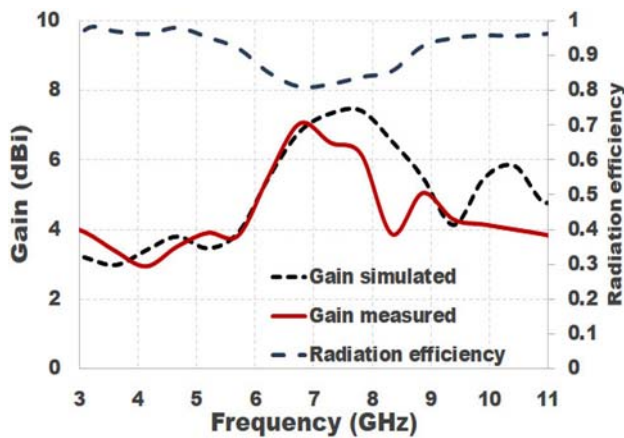


**Figure 8.** Measured and simulated gain, and simulated radiation efficiency.

between both simulated and measured results and peak gain is reported as 7.2 dB. Further, it gives stable and good performance across the entire UWB range, which makes it a powerful candidate for various UWB applications.

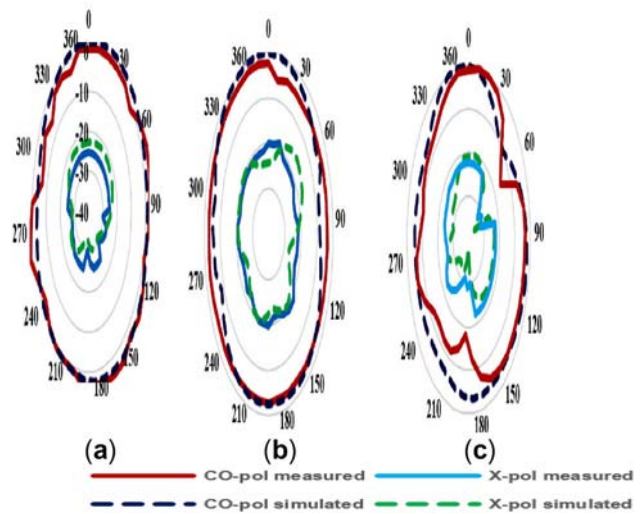


**Figure 9.** Simulated and measured co and X polarization pattern of antenna A. 4.1 GHz, B. 6.2 GHz, C. 8.1 GHz.

**Acknowledgement**

Authors are thankful to prof. M V Kartikeyan, IIT Roorkee, India for providing the support in antenna measurement.

**References**

- [1] Ryu K S and Kishk A A 2003 Ultrawideband dielectric resonator antenna with broadside patterns mounted on a vertical ground plane edge. *IEEE Transactions on Antennas and Propagation* 58: 1047–1053
- [2] Abedian M, Rahim S K, Danesh S, Hakimi S, Cheong L Y and Jamaluddin M H 2014 Novel design of compact UWB dielectric resonator antenna with dual-band-rejection characteristics for WiMAX/WLAN bands. *IEEE Antennas and Wireless Propagation Letters* 14: 245–248
- [3] Luk K M and Leung K W 2003 *Dielectric Resonator Antenna*. U. K.: Research Studies Press, UK
- [4] Yaduvanshi R S and Parthasarathy H 2016 *Rectangular dielectric resonator antennas*. Berlin: Springer. 18–78
- [5] McAllister M W, Long S A, and Conway G L 1983 Rectangular dielectric resonator antenna. *Electronics Letters* 19(6): 218–219
- [6] Lim E H, Leung K W and Fang X S 2010 The compact circularly-polarized hollow rectangular dielectric resonator antenna with an underlaid quadrature coupler. *IEEE Transactions on Antennas and Propagation*, 59(1): 288–293

- [7] Iqbal J, Illahi U, Sulaiman M I, Alam M and Mazliham M S 2017 Circularly polarized bandwidth enhancement using hollow cylindrical DRA. In: *International Conference on Engineering Technology and Technopreneurship (ICE2T)*, 1–4
- [8] Kai L and Leung KW 2011 Wideband circularly polarized hollow dielectric resonator antenna with a parasitic strip. In: *Proceedings of 2011 Cross-Strait Quad-Regional Radio Science and Wireless Technology Conference* 1: 514–515
- [9] Sharma A, Sarkar A, Biswas A and Akhtar M J 2018 A-shaped wideband dielectric resonator antenna for wireless communication systems and its MIMO implementation. *International Journal of RF and Microwave Computer-Aided Engineering* 28(8): e21402
- [10] Makwana G D, Ghodgaonkar D and Gupta S 2015 Dual mode and miniaturized rectangular dielectric resonator antenna with a simple feeding scheme. *International Journal of RF and Microwave Computer-Aided Engineering* 25(3): 229–235
- [11] Kshirsagar P, Gupta S and Mukherjee B 2018 A two-segment rectangular dielectric resonator antenna for ultra-wideband application. *Electromagnetics* 38(1): 20–33
- [12] Fakhte S, Oraizi H, Karimian R, and Fakhte R 2015 A new wideband circularly polarized stair-shaped dielectric resonator antenna. *IEEE Transactions on Antennas and Propagation* 63(4): 1828–1832
- [13] Varshney G, Gotra S, Pandey V S and Yaduvanshi R S 2018 Inverted-sigmoid shaped multiband dielectric resonator antenna with dual-band circular polarization. *IEEE Transactions on Antennas and Propagation* 66(4): 2067–2072
- [14] Kumar R and Chaudhary R K 2019 A dual-band dual-polarized cubical DRA coupled with a new modified cross-shaped slot for ISM (2.4 GHz) and Wi-MAX (3.3-3.6 GHz) band applications. *International Journal of RF and Microwave Computer-Aided Engineering* 29(1): e21449
- [15] Pan Y M, Leung K W and Luk K M 2011 Design of the millimeter-wave rectangular dielectric resonator antenna using a higher-order mode. *IEEE Transactions on Antennas and Propagation* 59(8): 2780–2788
- [16] Denidni T A and Weng Z 2011 Hybrid ultrawideband dielectric resonator antenna and band-notched designs. *IET Microwaves, Antenna & Propagation* 5(4): 450–458